BIOCHEMISTRY
including biophysical chemistry & molecular biology

Article

pubs.acs.org/biochemistry

Lipid-Induced Conformational Changes within the Cytochrome b_6f Complex of Oxygenic Photosynthesis

S. Saif Hasan,[†] Jason T. Stofleth,[†,‡] Eiki Yamashita,[§] and William A. Cramer*[,†]

[†]Department of Biological Sciences, Purdue University, West Lafayette, Indiana 47907, United States

[‡]Department of Chemistry and Biochemistry, University of California, San Diego, California 92037, United States

[§]Institute for Protein Research, Osaka University, Osaka, Japan

Supporting Information

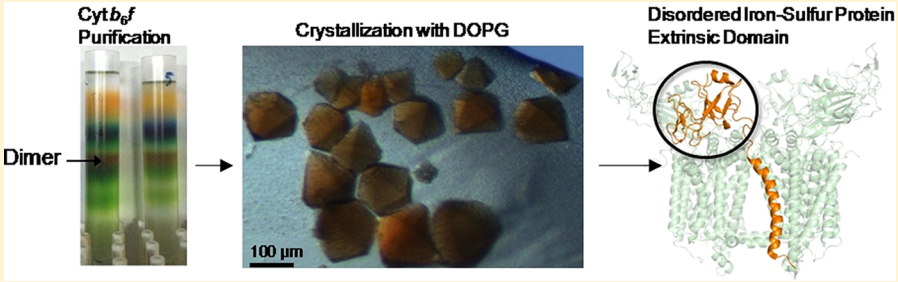

ABSTRACT: Cytochrome b_6f catalyzes quinone redox reactions within photosynthetic membranes to generate a transmembrane proton electrochemical gradient for ATP synthesis. A key step involves the transfer of an electron from the [2Fe-2S] cluster of the iron−sulfur protein (ISP) extrinsic domain to the cytochrome *f* heme across a distance of 26 Å, which is too large for competent electron transfer but could be bridged by translation−rotation of the ISP. Here we report the first crystallographic evidence of significant motion of the ISP extrinsic domain. It is inferred that extensive crystallographic disorder of the ISP extrinsic domain indicates conformational flexibility. The ISP disorder observed in this structure, in contrast to the largely ordered ISP structure observed in the b_6f complex supplemented with neutral lipids, is attributed to electrostatic interactions arising from anionic lipids.

The cytochrome b_6f complex (cyt b_6f) (Figure 1) of oxygenic photosynthesis, along with the cytochrome bc_1 complex in the respiratory chain and purple photosynthetic bacteria, belongs to the hetero-oligomeric family of transmembrane cytochrome *bc* complexes.[1,2] Cyt *bc* complexes share extensive structural and functional homology.[2−5] Together, these complexes catalyze proton-coupled electron transfer reactions of the substrate quinone or quinol to generate a transmembrane proton electrochemical gradient that is utilized for ATP synthesis.[5] On the electrochemically positive (p) side of the membrane, an electron is transferred from the substrate quinol, bound within the transmembrane p-side quinol oxidation (Q_p) site, to the [2Fe-2S] cluster of the iron−sulfur protein (ISP) extrinsic domain. The electron is then transferred to the extrinsic heme for c_1 in the b_6f or bc_1 complex, where it is utilized for the reduction of $NADP^+$ and O_2.

Crystal structures of the cyt b_6f complex show that the ISP [2Fe-2S] cluster is separated from the extrinsic heme *f* by ∼26 Å.[6−10] Direct transfer of electrons from the [2Fe-2S] cluster to heme *f* would then be expected to proceed at a rate that is orders of magnitude slower than required physiologically.[11] In the cyt bc_1 complex, electron transfer rates are accelerated by a large-scale domain motion of the ISP extrinsic domain that bridges the distance to the heme of cyt c_1.[12] On the basis of the homology between cyt *bc* complexes, it is expected that the cyt b_6f ISP extrinsic domain must also undergo conformational changes to transfer electrons from the membrane extrinsic quinol to the cyt *f* heme.[4,6] However, crystal structures of the cyt b_6f complex obtained in the presence of quinone analogue inhibitors have thus far not revealed evidence of large-scale changes in the position of the ISP extrinsic domain.[6,7,9,10] Although cyt *f* in the b_6f complex and cyt c_1 of the bc_1 complex each act as the electron acceptor for the [2Fe-2S] cluster in the ISP extrinsic domain, the structure of the extrinsic domains of cyt *f* and cyt c_1 is not conserved and is markedly different.[13,14] The extrinsic domain of cyt *f* consists of a 75 Å elongated β-sheet (Figures 2A, B), while the cyt c_1 extrinsic domain is more compact and predominantly α-helical (Figure 2C, D). Therefore, the structural barrier provided by the extrinsic domain of cyt *f* and cyt c_1 to motion of the ISP extrinsic domain is different.[6,15] The elongated structure of the cyt *f* extrinsic domain restricts the space available for ISP conformational changes, which are required to move the [2Fe-2S] cluster of the ISP extrinsic domain from a membrane proximal location to a cyt *f* proximal position. Neither the nature of conformational changes undergone by the ISP extrinsic domain during electron

Received: December 6, 2012
Revised: January 31, 2013
Published: March 20, 2013

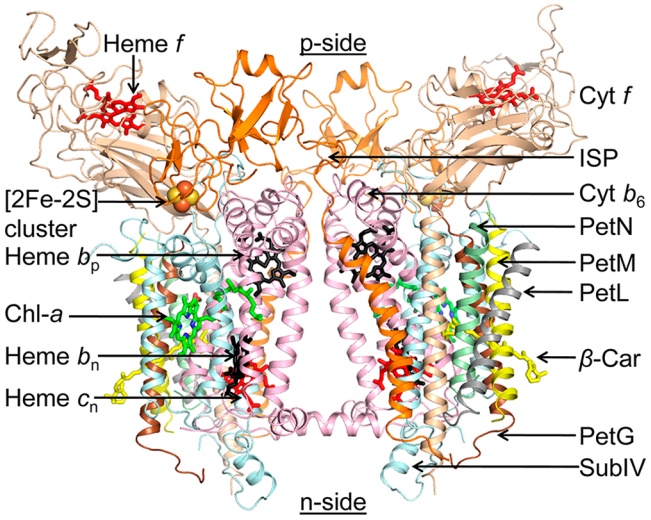

Figure 1. Cyt b_6f complex from the moderately thermophilic cyanobacterium *Mastigocladus laminosus* (PDB entry 2E74). Polypeptide subunits are shown as ribbons and prosthetic groups as sticks and spheres: pink for cytochrome b_6 (cyt b_6), cyan for subunit IV (subIV), wheat for cytochrome *f* (cyt *f*), orange for iron−sulfur protein (ISP), brown for Pet G, gray for Pet L, yellow for Pet M, and green for Pet N.

transfer by the b_6f complex nor the local driving force for the redox-linked conformational change is known. Hence, understanding of redox-linked ISP conformational changes within the cyt b_6f complex has remained relatively limited. Utilizing a new 2.80 Å crystal structure of the cyt b_6f complex isolated from the moderately thermophilic filamentous cyanobacterium *Mastigocladus laminosus* (PDB entry 4I7Z), we present evidence of the extrinsic domain flexibility of the ISP in the b_6f complex.

MATERIALS AND METHODS

Protein Purification. *M. laminosus* thylakoid membranes were prepared as described previously.[16,17] Cyt b_6f was purified from the membranes with minor modifications to the purification protocol. Briefly, after β-octyl glucoside-mediated (Anatrace) and sodium cholate-mediated (Sigma-Aldrich) extraction of the protein from thylakoid membranes, and partial purification by ammonium sulfate precipitation and hydrophobic interaction chromatography using a propyl-agarose resin, the protein that eluted from the hydrophobic column was concentrated to 4.8 mL and loaded on six sucrose density gradient tubes [~10 mL per tube of 10−32% sucrose in 30 mM Tris-HCl (pH 7.5) at 4 °C, 50 mM NaCl, 5 mM $MgCl_2$, 5 mM KCl, 1 mM EDTA, 6 mM 6-aminocaproic acid and benzamidine, and 0.05% solubility-grade UDM (Anatrace)]. Following two sucrose density gradient centrifugation steps [16 h, 36000 rpm (SW-41 rotor, Beckman), 4 °C], pure cyt b_6f dimer was pooled and concentrated in an Amicon-4 concentrator (100000 nominal molecular weight cutoff) to ~200 μL. The protein buffer was exchanged with 30 mM Tris-HCl (pH 7.5) (pH equilibrated at room temperature, ~25 °C), 50 mM NaCl, 10% sucrose, and 0.05% analytical-grade UDM (Anatrace) (TNS-UDM buffer) at 4 °C. The buffer was then exchanged with TNS and 0.15% UDM supplemented with 1.8 mM DOPG. The protein was concentrated to 135−180 μM. The DOPG-containing buffer for protein crystallization was prepared from a DOPG lipid stock (25 mg/mL, Avanti Polar Lipids) in organic solvent; 200 μL of the lipid was dried in a glass test tube under a nitrogen stream and then left overnight in a desiccator. The dried lipid was suspended in TNS buffer by gentle vortexing. Analytical-grade UDM (Anatrace) was added to a final concentration of 0.15% (w/v), and the buffer was

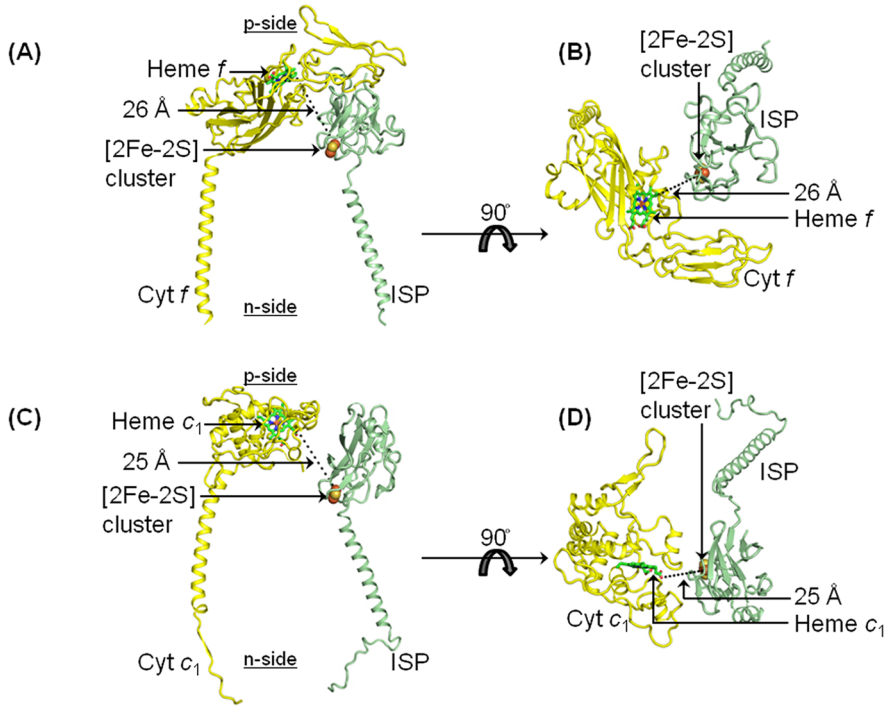

Figure 2. p-Side extrinsic domain architecture of the cyt b_6f (PDB entry 2E74) and bc_1 complex (PDB entry 3CX5). (A and B) The cyt *f* extrinsic domain (yellow) consists of an elongated β-sheet structure that extends over 75 Å. (C and D) In contrast, the cyt c_1 extrinsic domain (yellow) is predominantly α-helical in structure and is more compact. The ISP polypeptide is colored pale green, the heme of cyt *f* or cyt c_1 green or red, respectively (sticks), and the ISP [2Fe-2S] cluster as brown/wheat spheres.

dx.doi.org/10.1021/bi301638h | *Biochemistry* 2013, 52, 2649−2654

frozen and thawed in liquid nitrogen 15 times. The clarified buffer containing the DOPG lipid was then sonicated in a water bath (20 min, room temperature). The buffer (1.8 mM DOPG) was cooled to 4 °C prior to protein buffer exchange.

Protein Crystallization and Cryo-Freezing. Cyt b_6f was crystallized as described previously,[10] with minor modifications. Briefly, 1.5 μL of the protein (135−180 μM) was mixed with an equal volume of the reservoir solution [100 mM Tris-HCl (pH 8.5) at room temperature, 200 mM $MgCl_2$, 40 mM $CdCl_2$, and 16−17% PEG-550 MME] at 4 °C. Hexagonal bipyramidal crystals appeared in 24−36 h at 4 °C through hanging drop vapor diffusion and grew to a size of 100−150 μm in the largest dimension (Figure S1 of the Supporting Information). For cryo-protection, after 5−7 days, crystals harvested from the 16% PEG 550 MME droplet were transferred to a cryo-protection buffer [500 μL of 100 mM Tris-HCl (pH 8.5) (pH equilibrated at room temperature), 200 mM $MgCl_2$, 40 mM $CdCl_2$, 21% PEG 550 MME, 0.15% UDM (analytical-grade), and 0.18 mM DOPG] in a sealed chamber for 30 min at 4 °C; 250 μL of the buffer was then removed and replaced by an equal volume of the same buffer supplemented with 5% glycerol. The glycerol concentration was increased gradually to 25%, after which the crystals were flash-frozen in liquid nitrogen.

X-ray Data Collection, Data Reduction, and Structure Solution. Diffraction data sets were collected under cryo-conditions (100 K) at beamline 23-ID-B of the Advanced Photon Source (Argonne National Laboratory, Argonne, IL). Data reduction and scaling were performed in the HKL2000 suite[18] to $\langle I\rangle/\langle\sigma_I\rangle \approx 2$ in the highest-resolution shell. Negative reflections were omitted during scaling. Diffraction data sets from two crystals were merged together to increase completeness. Rigid body refinement was performed in REFMAC5,[19] using an initial monomeric polypeptide model of the *M. laminosus* cyt b_6f complex (PDB entry 2E74).[10] Prosthetic groups, lipids, detergents, and water molecules were built into the structure using Coot[20] followed by several cycles of restrained refinement in REFMAC5 and Phenix.[21] Table 1 summarizes the crystallographic structure statistics. Coordinates have been deposited in the Protein Data Bank as entry 4I7Z.

Structural Superposition. Coordinates of cyt b_6f crystal structures (PDB entries 2E74, 2E76, and 4I7Z) were superposed in PyMol (http://www.pymol.org). Fitting was performed using a pair-fit routine between the backbone C_α atoms of the cyt b_6 subunit (chain A) of PDB entries 2E76 and 2E74 (C_α root-mean-square deviation of 0.41 Å), and between PDB entries 2E76 and 4I7Z (C_α rmsd of 0.42 Å).

Identification of the ISP Docking Interface. Coordinates of the cyt b_6f structure (PDB entry 2E76) obtained in the presence of the quinone analogue inhibitor tridecyl-stigmatellin were analyzed with the Ligand-Protein Server.[22] An interaction distance cutoff of 4.0 Å was imposed to identify the ISP extrinsic domain residues (chain D, residues 109−179) that interact with the transmembrane ISP binding site formed by cytochrome b_6 (chain A, residues Trp146, Lys149, Ile150, and Val154) and subunit IV (chain B, Phe69, Thr71, Pro72, Leu73, Ile75, Phe85, Leu88, Arg89, Lys94, and Leu151). ISP extrinsic domain residues Thr109, His110, Leu111, Gly112, Cys113, Val114, Pro127, Cys128, His129, and Pro145 make contact with the residues of cyt b_6 and subIV.

Denaturing Electrophoresis. Purification of cyt b_6f from spinach thylakoid membranes and sodium dodecyl sulfate−polyacrylamide gel electrophoresis (SDS−PAGE) analysis was performed as described previously.[23] The purified protein was concentrated to 90 μM in the presence of Tris-HCl (100 mM, pH 7.5), NaCl (50 mM), and lipid (900 μM DOPG or DOPC, Avanti Polar Lipids); 10 μg of protein loaded in each well was separated by electrophoresis using a current of 12.5−15.0 mA.

Table 1. Crystallographic Data Summary for Cyt b_6f with DOPG[a]

Data Collection	
space group	$P6_122$
a, *b*, *c* (Å)	159.45, 159.45, 362.75
α, β, γ (deg)	90, 90, 120
resolution (Å)	50.00−2.80 (2.85−2.80)
R_{merge}	0.12 (0.45)
$\langle I\rangle/\langle\sigma_I\rangle$	15.6 (2.1)
completeness (%)	99.2 (94.7)
redundancy	9.3 (4.3)
Refinement	
resolution (Å)	48.52−2.80
no. of reflections	627305
R_{work}/R_{free}	0.247/0.271
rmsd	
bond lengths (Å)	0.003
bond angles (deg)	0.931

[a]Data merged from two crystals; values in parentheses correspond to the values for the outer shell.

RESULTS

The purified, delipidated *M. laminosus* cyt b_6f complex was cocrystallized with the physiological anionic lipid dioleoylphosphatidylglycerol (DOPG). Previous crystal structures of the cyt b_6f complex were obtained in the presence of either the synthetic neutral lipid dioleoylphosphatidylcholine (DOPC)[6,9,10] or native lipids,[7] which are predominantly neutral electrostatically[24,25] and have been found to be associated with an ordered ISP extrinsic domain. Unit cell parameters ($P6_122$, $a = b = 159.45$ Å, $c = 362.75$ Å, $\alpha = \beta = 90°$, $\gamma = 120°$) of the structure reported in this study were similar to those reported earlier for the *M. laminosus* cyt b_6f structure (PDB entry 2E74, $P6_122$, $a = b = 158.34$ Å, $c = 361.09$ Å, $\alpha = \beta = 90°$, $\gamma = 120°$) obtained in the presence of the neutral lipid DOPC.[10] Electron density was assigned to seven of the eight polypeptide subunits within the b_6f monomer, which constitute the crystallographic asymmetric unit of the DOPG-containing b_6f structure, with the exception of the ISP extrinsic domain. Electron density for the ISP was found to be incomplete beyond the p-side Ser46 residue of the ISP transmembrane helix (TMH).

A crystallographic structure analysis was performed to study the effect of lipid charge on the transmembrane docking surface for the ISP extrinsic domain. In the cyt bc_1 complex, transmembrane residues proximal to the Q_P site that form the ISP docking interface have been reported to undergo conformational changes upon binding of the ISP extrinsic domain.[26] The cyt b_6f ISP extrinsic domain is crystallographically defined in the presence of the neutral lipid DOPC in cyt b_6f structures obtained in the absence (PDB entry 2E74, resolution of 3.00 Å)[10] and presence (PDB entry 2E76, resolution of 3.43 Å)[10]of the quinone analogue inhibitor tridecyl-stigmatellin (TDS). In the presence of TDS, the ISP extrinsic domain is located closer to the transmembrane

dx.doi.org/10.1021/bi301638h | *Biochemistry* 2013, 52, 2649−2654

docking surface by approximately 3 Å.[4] It was found in this study that residues Thr109–Val114, Pro127–His129, and Pro145 of the ISP extrinsic domain (PDB entry 2E76) interact with the docking surface formed by the transmembrane cytochrome b_6 (cyt b_6) and subunit IV (subIV) polypeptides (shown in Figure 3). Conformational changes within the

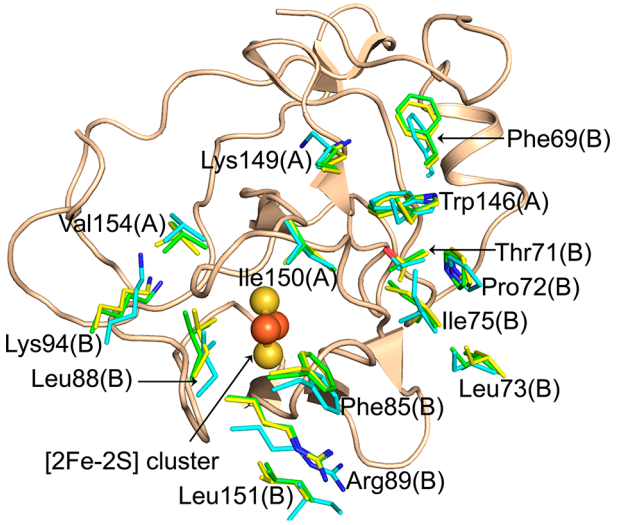

Figure 3. Docking interface for the ISP extrinsic domain. The figure was generated by superposition of three crystal structures of the cyt b_6f complex: PDB entries 2E74, 2E76, and 4I7Z (described in this study). Residues from cyt b_6 are identified as A and those of subIV as B. The ISP extrinsic domain is shown as wheat-colored ribbon and includes the [2Fe-2S] cluster. Residues are color-coded according to their respective crystal structures: yellow for PDB entry 2E74, cyan for PDB entry 2E76, and green for PDB entry 4I7Z. No large conformational changes are observed in the ISP docking interface.

surface for ISP docking are not detected by superposition of the DOPG-containing cyt b_6f structure with the cyt b_6f structure obtained with the neutral lipid DOPC (PDB entries 2E74 and 2E76), in contrast with cyt bc_1 where changes in the cyt b interface for ISP docking have been documented.[26]

The absence of detectable conformational changes in the ISP binding site of cyt b_6f in the presence of DOPC and DOPG raises the possibility that electrostatic interactions arising from lipid headgroup charge may cause conformational changes in the ISP extrinsic domain. The cyt b_6f crystal structure described in this study has revealed four lipid sites per monomer (Figure 4A). One natural acidic sulquinovosyldiacylglycerol (SQDG) molecule has been previously described on the electrochemically negative (n) side of the b_6f complex.[7,9,10,27] The SQDG lipid is involved in the stabilization of the ISP and cyt f TMH.[28] Three additional lipids were identified in this study and have been modeled as the acidic phosphatidylglycerol (PG). Two of the lipid sites have been described for the neutral lipid in the crystal structures of the cyanobacterial cyt b_6f complex.[9,10] The anionic PG lipid ("PG1") occupies an n-side niche between the F and G TMH of subIV (Figure 4B). The lipid in this site was modeled as a DOPC in previous b_6f structures.[9,10] A p-side lipid binding site is formed by the peripheral Pet subunits G, L, M, and N (Figure 4C), which overlaps with the DOPC binding site in the cyanobacterial cyt b_6f complex (PDB entries 2E74 and 2ZT9).[9,10] The PG lipid ("PG2") also overlaps with the natural monogalactosyldiacylglycerol (MGDG) lipid found in

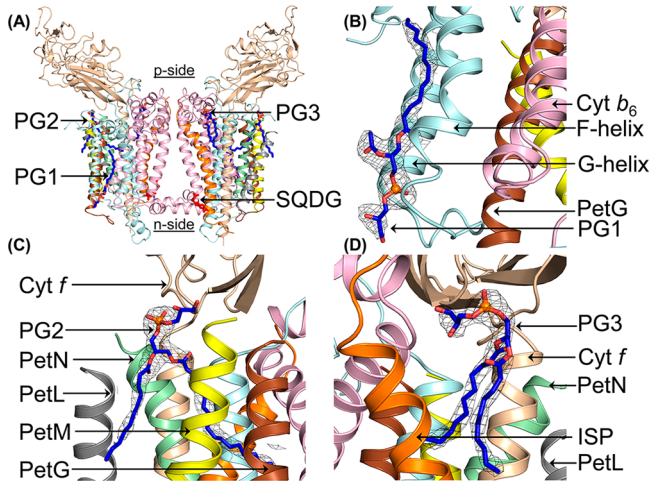

Figure 4. Anionic lipid binding sites in cyt b_6f. (A) Four anionic lipid sites in the b_6f complex. (B) PG1 bound between the F and G TMH of subIV. (C) PG2 inserted between peripheral Pet subunits. (D) PG3 located between the ISP and cyt f TMH. Mesh, $2F_o - F_c$ map, 1.2σ. The color code is the same as in Figure 1.

the cyt b_6f structure obtained from *Chlamydomonas reinhardtii* (PDB entry 1Q90).[7]

A novel PG site ("PG3") is located on the p-side between the ISP and cyt f TMHs (Figure 4D). The ligand in this site was modeled as a detergent molecule in previously published cyanobacterial cyt b_6f crystal structures (PDB entries 2E74 and 2ZT9)[9,10] and as the photosynthetic pigment eicosane in the *C. reinhardtii* cyt b_6f structure.[7] This lipid binding site shows conservation of location with the yeast respiratory cyt bc_1 complex (PDB entry 3CX5). An anionic phosphatidic acid (PA) lipid occupies a similar site in the cyt bc_1 complex.[29] It has been suggested that PA stabilizes the ISP TMH, while the extrinsic domain undergoes motion during catalysis.[30] This lipid-occupied site may be directly involved in lipid-mediated modulation of enzymatic activity in cyt bc complexes.

The thylakoid membrane consists predominantly of neutral lipids.[24,25] Anionic lipids form only a minor component and are restricted to the n-side leaflet of the thylakoid membrane bilayer.[25] In an environment of predominantly anionic lipids, as provided in the crystallization solution, the stability of the cyt b_6f complex may be affected, leading to the loss of the ISP extrinsic domain. Under such experimental conditions, the incomplete density of the ISP extrinsic domain can be attributed to secondary factors other than crystallographic disorder, such as proteolysis. To test the effect of anionic lipids on the stability of the cyt b_6f complex, a denaturing SDS–PAGE analysis was performed. The four "large" subunits of the cyt b_6f complex, i.e., cyt f, cyt b_6, ISP, and subIV, do not show any shift in effective molecular weight (M_r) in the presence of the anionic lipid DOPG compared to the M_r of subunits observed in the presence of the neutral lipid DOPC (Figure 5). It is inferred that the intra-membrane domain of the b_6f complex is stable upon interaction with DOPG.

DISCUSSION

Examples of functions or structural roles of anionic lipids in the structure and function of membrane proteins have been documented and discussed.[30,31] The SQDG molecule in cyt b_6f has been shown to be involved in assembly and stability.[28] In the Photosystem II complex, SQDG contributes to biological

dx.doi.org/10.1021/bi301638h | *Biochemistry* 2013, 52, 2649–2654

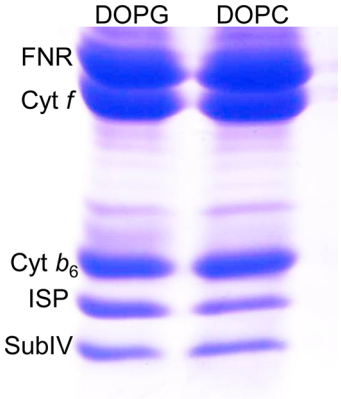

Figure 5. Lipid dependence of the stability of the purified cyt b_6f complex in lipids. The purified cyt b_6f complex from spinach thylakoid membranes was reconstituted with a lipid (DOPG or DOPC) at a molar ratio (protein:lipid) of 1:10. The molecular weight of the ISP subunit does not undergo a change in the presence of the anionic lipid DOPG, thereby indicating that the polypeptide remains intact in the presence of the anionic lipid. The band for the enzyme FNR, which is copurified with the spinach cyt b_6f complex, is also shown.

activity.[32−34] Mutants that lack SQDG demonstrate a normal content of Photosystem II, but with reduced activity that is restored by the addition of exogenous SQDG.[33] Similarly, a PG molecule may participate directly in modulating the kinetics of the bifurcated electron transfer pathway within the Photosystem I complex.[35,36] In the cyt b_6f structure described here, while none of the four lipid binding sites comes into direct contact with the ISP extrinsic domain, the absence of a well-defined electron density for this domain in the anionic lipid environment indicates that the electrostatic influence of the charge on the lipid headgroup may be involved in the binding of the ISP extrinsic domain at the p-side transmembrane docking site. The dielectric constant of the environment around the acidic lipids on the p-side and the ISP extrinsic domain docking site is expected to be much lower[37] than the bulk water dielectric constant of 81, which would permit the propagation of electrostatic interactions that alter the ISP binding properties of the docking surface and the ISP extrinsic domain itself. Perhaps because of limitations of resolution (2.80−3.43 Å), such conformational . changes in the intra-membrane domain have not been detected.

The conformational flexibility of the cyt b_6f ISP subunit has been a subject of debate. Mutagenesis of the ISP flexible hinge showed that the ISP is less susceptible to mutagenesis in cyt b_6f than in cyt bc_1.[28,38] This may be a consequence of the greater flexibility of the polyglycine hinge in the cyt b_6f complex than of the polyalanine hinge in bc_1. The hinge region is crystallographically disordered in the b_6f complex,[9,10] while its electron density is traced in the bc_1 complex (for example, in ref 39), thereby indicating larger flexibility of the ISP extrinsic domain in the b_6f complex. In the presence of the neutral lipid DOPC, the cyt b_6f ISP extrinsic domain is docked proximal to the transmembrane segment.[9,10] From the study presented here, it is suggested that the conformational flexibility of the ISP is a function of the lipid environment. Neutral and anionic lipids may be involved in modulating the extent of motion of the ISP extrinsic domain. From the b_6f structures obtained with the neutral lipid DOPC,[9,10] it is inferred that the ISP extrinsic domain in *situ* is tethered in a membrane proximal position.

It is significant to note that thylakoid membrane anionic lipids are predominantly restricted to the n-side leaflet.[25] The sidedness of lipids in crystal structures of photosynthetic membrane protein complexes follows their distribution in membranes.[30] A tightly bound PG molecule has been identified in the purified cyt b_6f, although the lipid is not observed in crystal structures.[27] Because the ISP extrinsic domain is located on the p-side, it is important to note the possibility of transmembrane communication between an n-side lipid and the membrane-bound ISP extrinsic domain through the low-dielectric transmembrane domain of the cyt b_6f complex. Further insights into lipid-induced conformational changes may be derived in the future from cyt b_6f crystal structures obtained at higher resolution.

■ ASSOCIATED CONTENT

Ⓢ Supporting Information

Crystals of the cyt b_6f complex from *M. laminosus* obtained in the presence of the anionic lipid DOPG, where the crystal morphology is different from that observed previously for *M. laminosus* cyt b_6f crystals supplemented with the neutral lipid DOPC. This material is available free of charge via the Internet at http://pubs.acs.org.

■ AUTHOR INFORMATION

Corresponding Author

*E-mail: waclab@purdue.edu. Phone: (765) 494-4956.

Funding

Financial support was provided by National Institutes of Health Grant GM-038323 and the Henry Koffler Distinguished Professorship (W.A.C.) and Purdue University (S.S.H.).

Notes

The authors declare no competing financial interest.

■ ACKNOWLEDGMENTS

We thank P. Afonine, R. Agarwal, J. T. Bolin, S. Kumar, P. Plevka, C. B. Post, V. M. Prasad, M. G. Rossmann, S. Savikhin, and T. Schmidt for discussions, S. Corcoran (beamline 23-ID-B), J. Chen, and M. Oldham (Purdue University) for advice on diffraction data collection, and the CCP4 workshop 2010 for advice on structure solution.

■ ABBREVIATIONS

β-Car, β-carotene; Chl-*a*, chlorophyll *a*; cyt, cytochrome; DOPC, dioleoylphosphatidylcholine (neutral lipid); DOPG, dioleoylphosphatidylglycerol (anionic lipid); FNR, ferredoxin-NAD(P)$^+$-oxidoreductase; ISP, Rieske iron−sulfur protein; MGDG, monogalactosyldiacylglycerol (neutral lipid); M_r, molecular weight; n- and p-side, electrochemically negative and positive sides, respectively, of the membrane; PA, phosphatidic acid (anionic lipid); PDB, Protein Data Bank; PG, phosphatidylglycerol (anionic lipid); Q_p site, quinol oxidation site; rmsd, root-mean-square deviation; SQDG, sulfoquinovosyldiacylglycerol (anionic lipid); subIV, subunit IV; TDS, tridecyl-stigmatellin; TMH, transmembrane helix; TNS, Tris-NaCl-sucrose buffer; UDM, *n*-undecyl β-D-maltopyranoside.

■ REFERENCES

(1) Schutz, M., Brugna, M., Lebrun, E., Baymann, F., Huber, R., Stetter, K. O., Hauska, G., Toci, R., Lemesle-Meunier, D., Tron, P.,

Schmidt, C., and Nitschke, W. (2000) Early evolution of cytochrome bc complexes. *J. Mol. Biol. 300*, 663−675.
(2) Darrouzet, E., Cooley, J. W., and Daldal, F. (2004) The Cytochrome bc_1 Complex and its Homologue the b_6f Complex: Similarities and Differences. *Photosynth. Res. 79*, 25−44.
(3) Widger, W. R., Cramer, W. A., Herrmann, R. G., and Trebst, A. (1984) Sequence homology and structural similarity between cytochrome b of mitochondrial complex III and the chloroplast b6-f complex: Position of the cytochrome b hemes in the membrane. *Proc. Natl. Acad. Sci. U.S.A. 81*, 674−678.
(4) Cramer, W. A., Hasan, S. S., and Yamashita, E. (2011) The Q cycle of cytochrome bc complexes: A structure perspective. *Biochim. Biophys. Acta 1807*, 788−802.
(5) Berry, E. A., Guergova-Kuras, M., Huang, L. S., and Crofts, A. R. (2000) Structure and function of cytochrome bc complexes. *Annu. Rev. Biochem. 69*, 1005−1075.
(6) Kurisu, G., Zhang, H., Smith, J. L., and Cramer, W. A. (2003) Structure of the cytochrome b6f complex of oxygenic photosynthesis: Tuning the cavity. *Science 302*, 1009−1014.
(7) Stroebel, D., Choquet, Y., Popot, J. L., and Picot, D. (2003) An atypical haem in the cytochrome b_6f complex. *Nature 426*, 413−418.
(8) Yan, J. S., Kurisu, G., and Cramer, W. A. (2006) Intraprotein transfer of the quinone analogue inhibitor 2,5-dibromo-3-methyl-6-isopropyl-p-benzoquinone in the cytochrome b_6f complex. *Proc. Natl. Acad. Sci. U.S.A. 103*, 69−74.
(9) Baniulis, D., Yamashita, E., Whitelegge, J. P., Zatsman, A. I., Hendrich, M. P., Hasan, S. S., Ryan, C. M., and Cramer, W. A. (2009) Structure-Function, Stability, and Chemical Modification of the Cyanobacterial Cytochrome b6f Complex from *Nostoc* sp. PCC 7120. *J. Biol. Chem. 284*, 9861−9869.
(10) Yamashita, E., Zhang, H., and Cramer, W. A. (2007) Structure of the cytochrome b6f complex: Quinone analogue inhibitors as ligands of heme cn. *J. Mol. Biol. 370*, 39−52.
(11) Moser, C. C., Keske, J. M., Warncke, K., Farid, R. S., and Dutton, P. L. (1992) Nature of biological electron transfer. *Nature 355*, 796−802.
(12) Zhang, Z., Huang, L., Shulmeister, V. M., Chi, Y. I., Kim, K. K., Hung, L. W., Crofts, A. R., Berry, E. A., and Kim, S. H. (1998) Electron transfer by domain movement in cytochrome bc1. *Nature 392*, 677−684.
(13) Carrell, C. J., Schlarb, B. G., Bendall, D. S., Howe, C. J., Cramer, W. A., and Smith, J. L. (1999) Structure of the soluble domain of cytochrome f from the cyanobacterium *Phormidium laminosum*. *Biochemistry 38*, 9590−9599.
(14) Martinez, S. E., Huang, D., Szczepaniak, A., Cramer, W. A., and Smith, J. L. (1994) Crystal structure of chloroplast cytochrome f reveals a novel cytochrome fold and unexpected heme ligation. *Structure 2*, 95−105.
(15) Hasan, S. S., and Cramer, W. A. (2012) On rate limitations of electron transfer in the photosynthetic cytochrome b_6f complex. *Phys. Chem. Chem. Phys. 14*, 13853−13860.
(16) Zhang, H., Kurisu, G., Smith, J. L., and Cramer, W. A. (2003) A defined protein-detergent-lipid complex for crystallization of integral membrane proteins: The cytochrome b6f complex of oxygenic photosynthesis. *Proc. Natl. Acad. Sci. U.S.A. 100*, 5160−5163.
(17) Zhang, H., and Cramer, W. A. (2004) Purification and crystallization of the cytochrome b_6f complex in oxygenic photosynthesis. *Methods Mol. Biol. 274*, 67−78.
(18) Otwinowski, Z., and Minor, W. (1997) Processing of X-ray diffraction data collected in oscillation mode. *Methods Enzymol. 276*, 307−326.
(19) Murshudov, G. N., Skubak, P., Lebedev, A. A., Pannu, N. S., Steiner, R. A., Nicholls, R. A., Winn, M. D., Long, F., and Vagin, A. A. (2011) REFMAC5 for the refinement of macromolecular crystal structures. *Acta Crystallogr. D67*, 355−367.
(20) Emsley, P., Lohkamp, B., Scott, W. G., and Cowtan, K. (2010) Features and development of Coot. *Acta Crystallogr. D66*, 486−501.
(21) Adams, P. D., Afonine, P. V., Bunkoczi, G., Chen, V. B., Davis, I. W., Echols, N., Headd, J. J., Hung, L. W., Kapral, G. J., Grosse-Kunstleve, R. W., McCoy, A. J., Moriarty, N. W., Oeffner, R., Read, R. J., Richardson, D. C., Richardson, J. S., Terwilliger, T. C., and Zwart, P. H. (2010) PHENIX: A comprehensive Python-based system for macromolecular structure solution. *Acta Crystallogr. D66*, 213−221.
(22) Sobolev, V., Sorokine, A., Prilusky, J., Abola, E. E., and Edelman, M. (1999) Automated analysis of interatomic contacts in proteins. *Bioinformatics 15*, 327−332.
(23) Zhang, H., Whitelegge, J. P., and Cramer, W. A. (2001) Ferredoxin:$NADP^+$ oxidoreductase is a subunit of the chloroplast cytochrome b_6f complex. *J. Biol. Chem. 276*, 38159−38165.
(24) Gounaris, K., Barber, J., and Harwood, J. L. (1986) The thylakoid membranes of higher plant chloroplasts. *Biochem. J. 237*, 313−326.
(25) Gounaris, K., Sundby, C., Andersson, B., and Barber, J. (1983) Lateral heterogeneity of polar lipids in the thylakoid membranes of spinach chloroplasts. *FEBS Lett. 156*, 170−174.
(26) Crofts, A. R., Guergova-Kuras, M., Huang, L., Kuras, R., Zhang, Z., and Berry, E. A. (1999) Mechanism of ubiquinol oxidation by the bc_1 complex: Role of the iron sulfur protein and its mobility. *Biochemistry 38*, 15791−15806.
(27) Hasan, S. S., Yamashita, E., Ryan, C. M., Whitelegge, J. P., and Cramer, W. A. (2011) Conservation of lipid functions in cytochrome bc complexes. *J. Mol. Biol. 414*, 145−162.
(28) de Vitry, C., Ouyang, Y., Finazzi, G., Wollman, F. A., and Kallas, T. (2004) The chloroplast Rieske iron-sulfur protein. At the crossroad of electron transport and signal transduction. *J. Biol. Chem. 279*, 44621−44627.
(29) Lange, C., Nett, J. H., Trumpower, B. L., and Hunte, C. (2001) Specific roles of protein-phospholipid interactions in the yeast cytochrome bc1 complex structure. *EMBO J. 20*, 6591−6600.
(30) Palsdottir, H., and Hunte, C. (2004) Lipids in membrane protein structures. *Biochim. Biophys. Acta 1666*, 2−18.
(31) Jones, M. R. (2007) Lipids in photosynthetic reaction centres: Structural roles and functional holes. *Prog. Lipid Res. 46*, 56−87.
(32) Aoki, M., Sato, N., Meguro, A., and Tsuzuki, M. (2004) Differing involvement of sulfoquinovosyl diacylglycerol in photosystem II in two species of unicellular cyanobacteria. *Eur. J. Biochemistry 271*, 685−693.
(33) Sato, N. (2004) Roles of the acidic lipids sulfoquinovosyl diacylglycerol and phosphatidylglycerol in photosynthesis: Their specificity and evolution. *J. Plant Res. 117*, 495−505.
(34) Minoda, A., Sato, N., Nozaki, H., Okada, K., Takahashi, H., Sonoike, K., and Tsuzuki, M. (2002) Role of sulfoquinovosyl diacylglycerol for the maintenance of photosystem II in *Chlamydomonas reinhardtii*. *Eur. J. Biochem. 269*, 2353−2358.
(35) Fromme, P., Jordan, P., and Krauss, N. (2001) Structure of photosystem I. *Biochim. Biophys. Acta 1507*, 5−31.
(36) Grotjohann, I., and Fromme, P. (2005) Structure of cyanobacterial photosystem I. *Photosynth. Res. 85*, 51−72.
(37) White, S. H., and Wimley, W. C. (1999) Membrane protein folding and stability: Physical principles. *Annu. Rev. Biophys. Biomol. Struct. 28*, 319−365.
(38) Yan, J., and Cramer, W. A. (2003) Functional insensitivity of the cytochrome b6f complex to structure changes in the hinge region of the Rieske iron-sulfur protein. *J. Biol. Chem. 278*, 20925−20933.
(39) Solmaz, S. R., and Hunte, C. (2008) Structure of complex III with bound cytochrome c in reduced state and definition of a minimal core interface for electron transfer. *J. Biol. Chem. 283*, 17542−17549.